Technical Paper 1198

Wear of Single-Crystal Silicon Carbide in Contact With Various Metals in Vacuum

Kazuhisa Miyoshi and Donald H. Buckley

APRIL 1978

NASA

NASA Technical Paper 1198

Wear of Single-Crystal Silicon Carbide in Contact With Various Metals in Vacuum

Kazuhisa Miyoshi
Kanazawa University
Kanazawa, Japan

and

Donald H. Buckley
Lewis Research Center
Cleveland, Ohio

National Aeronautics
and Space Administration

Scientific and Technical Information Office

1978

The specimens were placed in the vacuum chamber, and the system was evacuated and subsequently baked out to obtain a pressure of 10^{-8} pascal (10^{-10} torr). When this pressure was obtained, argon gas was bled back into the vacuum chamber to a pressure of 1.3 pascals. A 1000-volt-direct-current potential was applied, and the specimens (both disk and rider) were argon sputter bombarded for 30 minutes. One hour after the sputtering operation was completed the vacuum chamber was reevacuated, and AES spectra of the disk surface were obtained to determine the degree of surface cleanliness. When the desired degree of cleanliness of disk surface was achieved, friction experiments were conducted (refs. 1 to 3).

Loads of 30 grams (0.29 N) were applied to the pin-disk contact. Both load and friction force were continuously monitored during a friction experiment. Sliding velocity was 3 millimeters per minute, with a total sliding distance of 2.5 millimeters. All friction experiments in vacuum were conducted with the system evacuated to a pressure of 10^{-8} pascal.

RESULTS AND DISCUSSION

Wear Behavior of Silicon Carbide

The sliding of a metal rider on silicon carbide results in cracks along cleavage planes of $\{10\bar{1}0\}$. Figure 1 shows scanning electron micrographs of the wear tracks on silicon carbide surfaces generated by 10 passes of the rhodium and copper riders. The cracks, which are observed in the wear tracks, primarily propagate along cleavage planes of $\{10\bar{1}0\}$. In figure 1(a) a hexagon-shaped light area at the beginning of the wear track is a large damaged area where the cracks were generated, propagated, and then intersected during loading and sliding by the rhodium rider. It is anticipated from figure 1(a) that subsurface-cleavage cracking of (0001) planes also occurs. Figure 1(b) indicates the surface cracking, observed on the side of the wear track, along cleavage planes of $\{10\bar{1}0\}$.

Figure 2 reveals the wear tracks for silicon carbide contacting titanium characterized by nearly complete hexagon-shaped pit. Wear debris particles (as seen in fig. 1) have been already ejected from the wear track. Again, the fracture is primarily due to the surface cracking of the $\{10\bar{1}0\}$ planes and the subsurface cracking of the (0001) planes, as anticipated, parallel to the interface. A scanning electron micrograph and an X-ray energy dispersive analysis for titanium on the silicon carbide surface are shown in figure 2. The concentrations of white spots in figure 2(b) correspond to those locations in figure 2(a) where titanium transfer is evident. A large amount of thin titanium film was seen around the hexagon-shaped pit in figure 2(a). These figures indicate that the cohesive bonds on both the silicon carbide and titanium surfaces fractured near the strong adhesive bonds at the interface.

In fact, the dislodged gross wear particle of silicon carbide, which was turned over, has a large amount of titanium on its back as shown in figure 3. Figure 3 shows a scanning electron micrograph and an X-ray energy-dispersive analysis of a silicon carbide wear track.

Figure 4 also reveals the dislodged gross wear debris observed on the sides of wear tracks on silicon carbide surfaces generated by 10 passes of the aluminum rider. Thus, fracture may readily occur in silicon carbide near the adhesive bond, and silicon carbide wear debris particles may be formed.

Nature of Interaction on Silicon Carbide Wear Debris

The wear scars on metals after sliding on silicon carbide surfaces may contain the silicon carbide wear debris. Figures 5 to 7 indicate that the wear debris of silicon carbide, produced in sliding on rhodium, copper, and cobalt, transferred to or was embedded in the metal riders. The wear debris generally slides or rolles on the metal surfaces and produces the indentations and deep grooves shown in figures 5 to 7. Figure 6 shows straight grooves, along the sliding direction on the metal, formed by the sliding of silicon carbide wear debris. Figure 7 also shows straight rows of indentations, along the sliding direction, formed by the rolling of silicon carbide wear debris.

On the other hand, figure 8 reveals that silicon carbide wear debris was produced and embedded in the metal by sliding, that it plowed the silicon carbide surface itself, and that the groove is produced in a plastic manner on the surface of silicon carbide. Generally, the silicon carbide wear debris surface is covered with metal film as indicated in the X-ray map of figure 8.

Wear Behavior of Metals

The wear scars on the metal riders after sliding against silicon carbide revealed a large number of plastically deformed grooves and indentations (which seem to depend on the nature of transfer of silicon carbide and the metal) formed primarily by the sliding and rolling of silicon carbide wear debris. (See fig. 9.) The less the chemical activity and the greater the resistance to shear of the metal, with the exception of rhodium and tungsten, the less the transfer to silicon carbide (ref. 1). (See tables I and II.) The wear scars are generally rougher with aluminum and titanium, which have much stronger chemical affinity and less resistance to shear than copper, nickel, cobalt, or iron. The wear scar of iron is much smoother, with fewer deep grooves and indentations (fig. 9(f)). The titanium wear scar has the roughest surface (fig. 10). This reflects the large amount of silicon carbide transfer to titanium. Figure 10 reveals that most of the large contact indentations contain silicon carbide wear debris.

Rhodium and tungsten have the greatest resistance to shear of the metals (see tables I and II) and produce and transfer lumps of wear particles (ref. 1). The wear scar on the rhodium rider (fig. 11) reveals evidence of fractured surface damage in addition to plastically deformed grooves and indentations primarily produced by sliding and rolling of silicon carbide wear debris. Further, with rhodium, a significant degree of cracking initiates in a grain boundary and extends along the grain boundaries of rhodium. Such a crack is shown in the micrograph of figure 12.

Figure 13, scanning electron micrographs of wear scars on the tungsten rider generated by 3 and 10 passes of the tungsten riders, reveals evidence of fractured surface damage and cracking along the grain boundary. In figure 13(a) the tungsten wear debris transferred back to the tungsten. The fracturing and cracking of rhodium and tungsten may be primarily due to the greater shear moduli of rhodium and tungsten.

CONCLUSIONS

As a result of observations of the wear behavior of single-crystal silicon carbide and metals in sliding contacts, the following conclusions are drawn:

(1) Metal riders sliding against single-crystal silicon carbide generate hexagon-shaped cracking and fracturing in the silicon carbide. This cracking and fracturing is believed to be due to cleavages of both prismatic and basal planes.

(2) The silicon carbide wear debris produced by brittle fracture during sliding, slides or rolls on both the metal and silicon carbide and produces grooves and indentations on these surfaces.

(3) The wear scars of the metals aluminum and titanium, which have much stronger chemical affinity for silicon and carbon, are generally rougher than those of other metals.

(4) The fracturing and cracking along the grain boundary of rhodium and tungsten observed may be primarily due to the greater shear moduli of these metals.

Lewis Research Center,
National Aeronautics and Space Administration,
Cleveland, Ohio, November 29, 1977,
506-16.

REFERENCES

1. Miyoshi, Kazuhisa; and Buckley, Donald H.: Friction and Metal-Transfer for Single-Crystal Silicon Carbide in Contact with Various Metals. NASA TP-1191, 1978.

2. Miyoshi, Kazuhisa; and Buckley, Donald H.: Friction and Fracture of Single-Crystal Silicon Carbide in Contact with Itself and Titanium. ASLE Transactions in process.

3. Miyoshi, Kazuhisa; and Buckley, Donald H.: Friction and Wear Behavior of Single-Crystal Silicon Carbide in Contact with Titanium. NASA TP-1035, 1977.

4. Gschneidner, Karl A., Jr.: Physical Properties and Interrelationships of Metallic and Semimetallic Elements. Solid State Physics, vol. 16, Frederick Seitz and David Turnbull, eds., Academic Press, 1965, pp. 275-426.

5. Drowart, J.; and De Maria, G.: Thermodynamic Study of the Binary System Carbon-Silicon Using a Mass Spectrometer. Silicon Carbide: A High Temperature Semiconductor, J. R. O'Connor and J. Smiltens, eds., Pergamon Press, 1960, pp. 16-23.

6. Carnahan, R. D.: Elastic Properties of Silicon Carbide. J. Am. Ceram. Soc., vol. 51, no. 4, Apr. 1968, pp. 223-224.

TABLE I. - CHARACTERISTICS OF METAL TRANSFER TO SINGLE-CRYSTAL SILICON CARBIDE (0001) SURFACE

[Transferred after 10 passes sliding +; not transferred after 10 passes sliding -; transferred after single pass sliding (+).]

The form of metal transfer	Al	Ti	Cu	Ni	Co	Fe	Rh	W	SiC[a]
Particle:									
Very small	+	+	+	+	+	+	+	+	+
Piled-up	+	+	+	+	+	+	-	-	-
Thin film:									
Streak	+	+	+	+	+	-	-	-	-
Multilayer (piled-up)	+	+	-	-	-	-	-	-	-
Lump	(+)	(+)	-	-	-	-	+	+	+

[a]Ref. 2.

TABLE II. - PHYSICAL PROPERTIES

Metal	Shear modulus (a)		Cohesive energy (a)	
	mPa	kg/cm^2	kJ/g·atom	kcal/g·atom
Al	26.6	0.271×10^{-6}	322	76.9
Ti	39.3	.401	469	112.2
Cu	45.1	.460	338	80.8
Ni	75.0	.765	428	102.3
Co	76.4	.779	426	101.7
Fe	81.5	.831	416	99.4
Rh	147	1.50	556	133.0
W	153	1.56	835.5	199.7
SiC	200	2.04	523	125

[a]Data from ref. 4 for metals and refs. 5 and 6 for SiC.

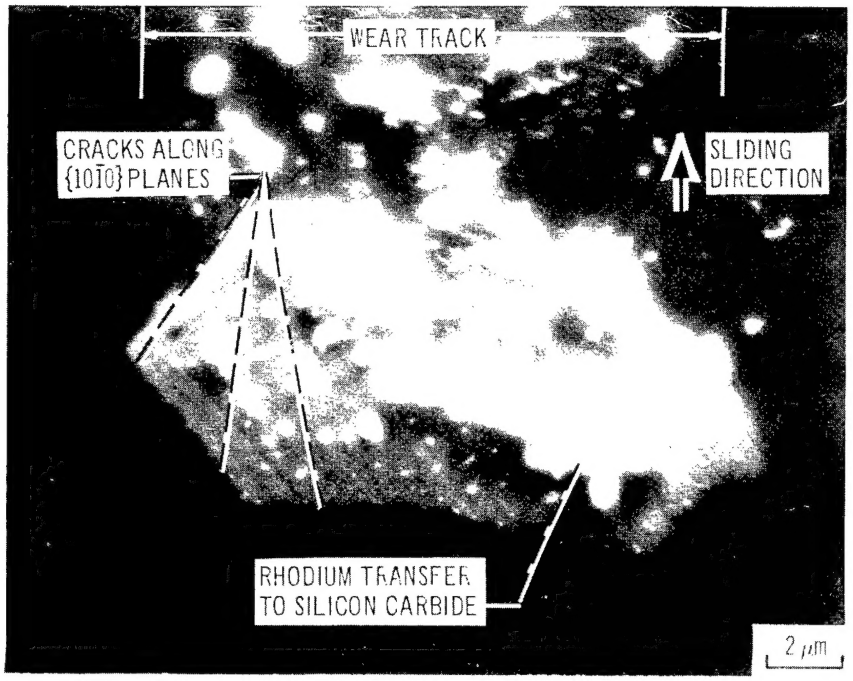

(a) Silicon carbide after contact with rhodium rider.

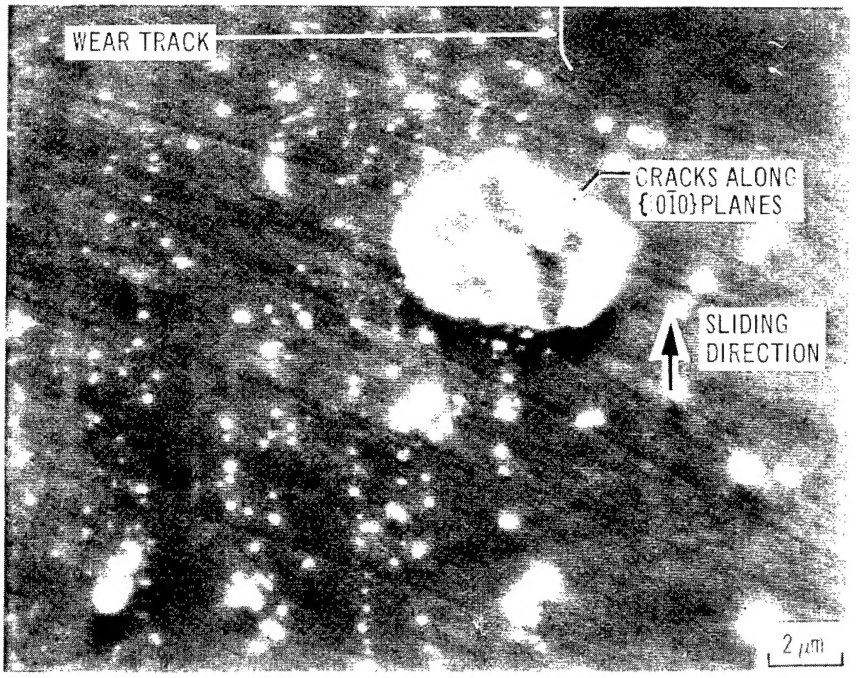

(b) Silicon carbide after contact with copper rider.

Figure 1. - Cracking of silicon carbide as result of sliding contact with metal riders. Ten passes on SiC (0001) surface; sliding direction, <10$\bar{1}$0>; sliding velocity, 3 mm/min; load, 30 g (0.29 N); temperature, 25° C; vacuum pressure, 10^{-8} Pa. (Scanning electron micrographs.)

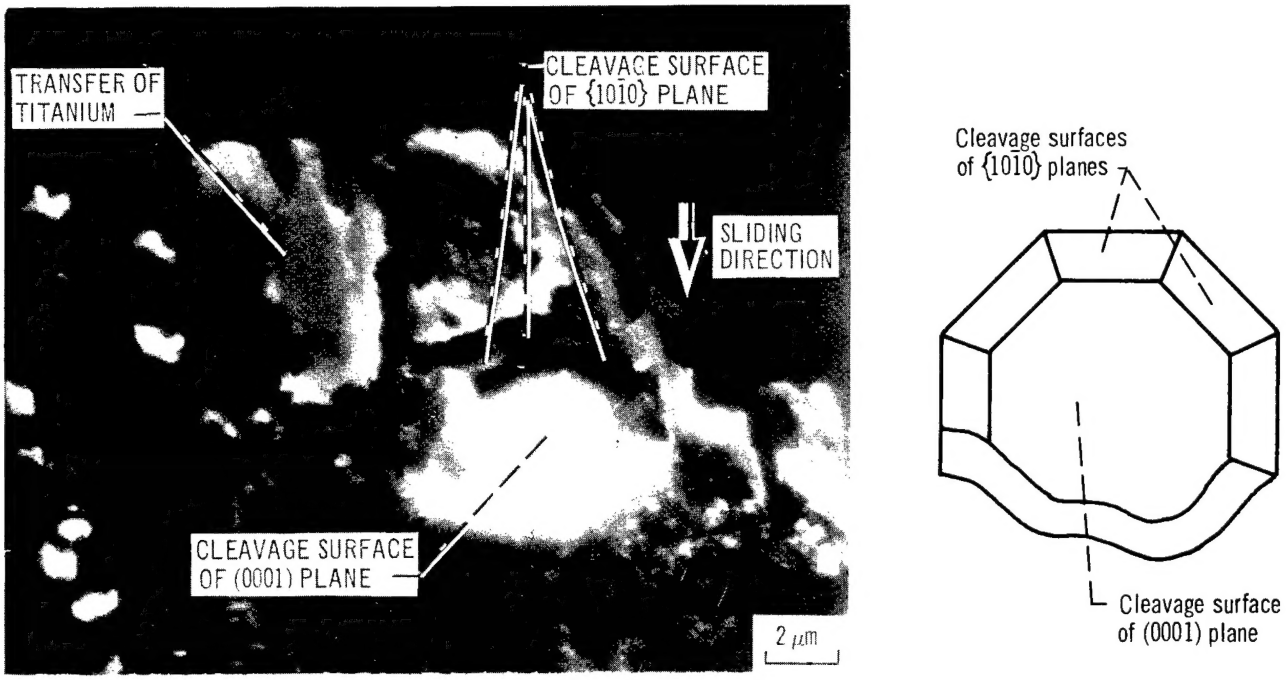

(a) Scanning electron micrograph.

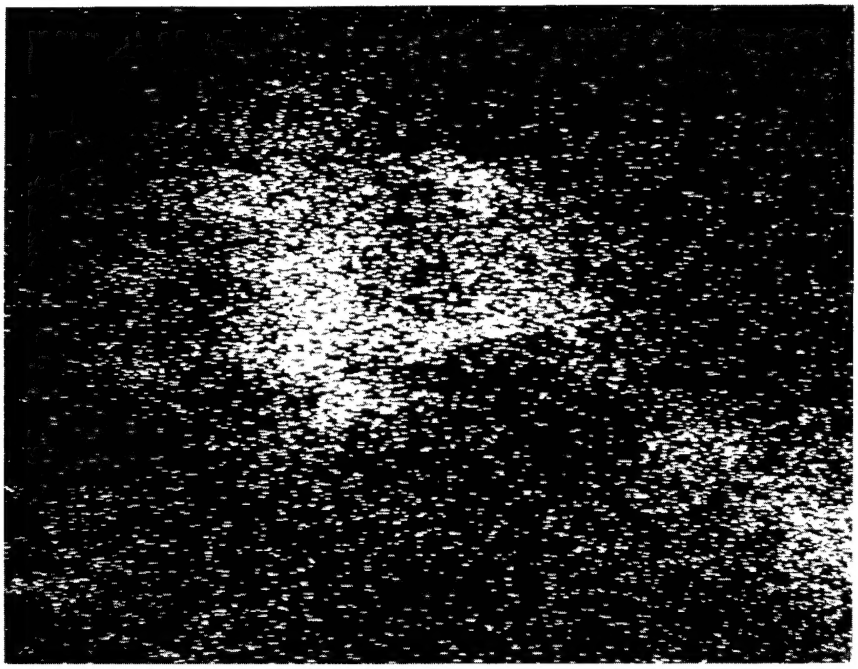

(b) Titanium K_α X-ray of silicon carbide; 1.5×10^4 counts.

Figure 2. - Hexagon shaped pit of silicon carbide as result of sliding contact with titanium rider. Ten passes on SiC (0001) surface; sliding direction, <10$\bar{1}$0>; sliding velocity, 3 mm/min; load, 30 g (0.29 N); temperature, 25° C; vacuum pressure, 10^{-8} Pa.

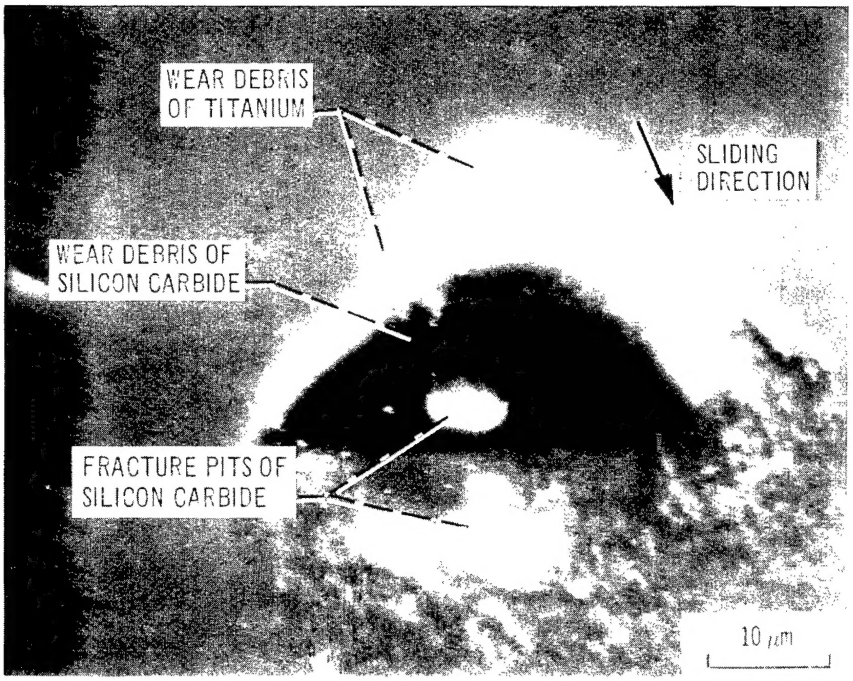

(a) Scanning electron micrograph.

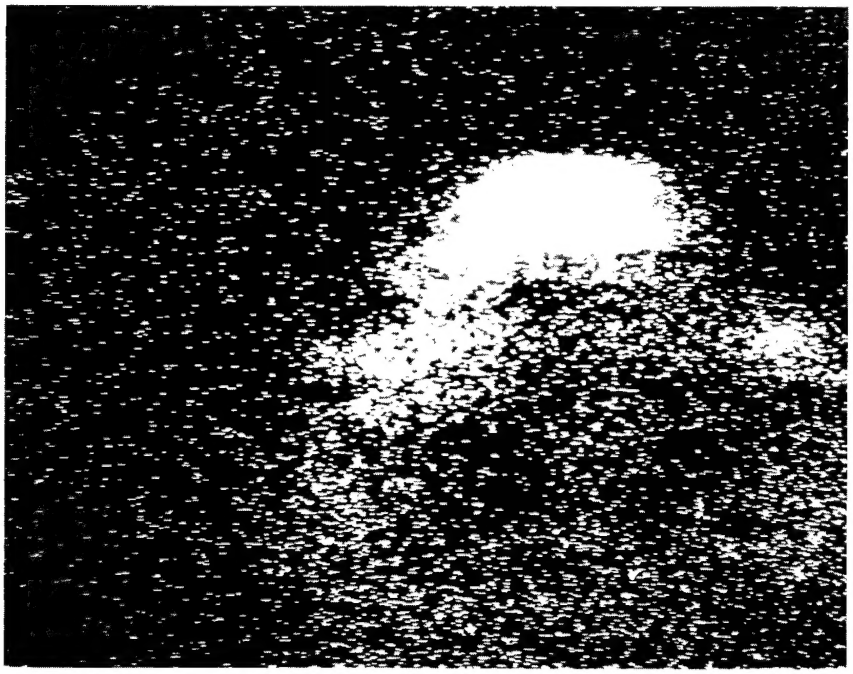

(b) Titanium K_α X-ray map of silicon carbide surface; 1.5×10^{-4} counts.

Figure 3. - Titanium and silicon carbide wear debris on SiC surface produced during sliding contact. Ten passes of Ti rider on SiC (0001) surface; sliding direction, $<10\bar{1}0>$; sliding velocity, 3 mm/min; load, 30 g (0.29 N); temperature, 25° C; vacuum pressure, 10^{-8} Pa.

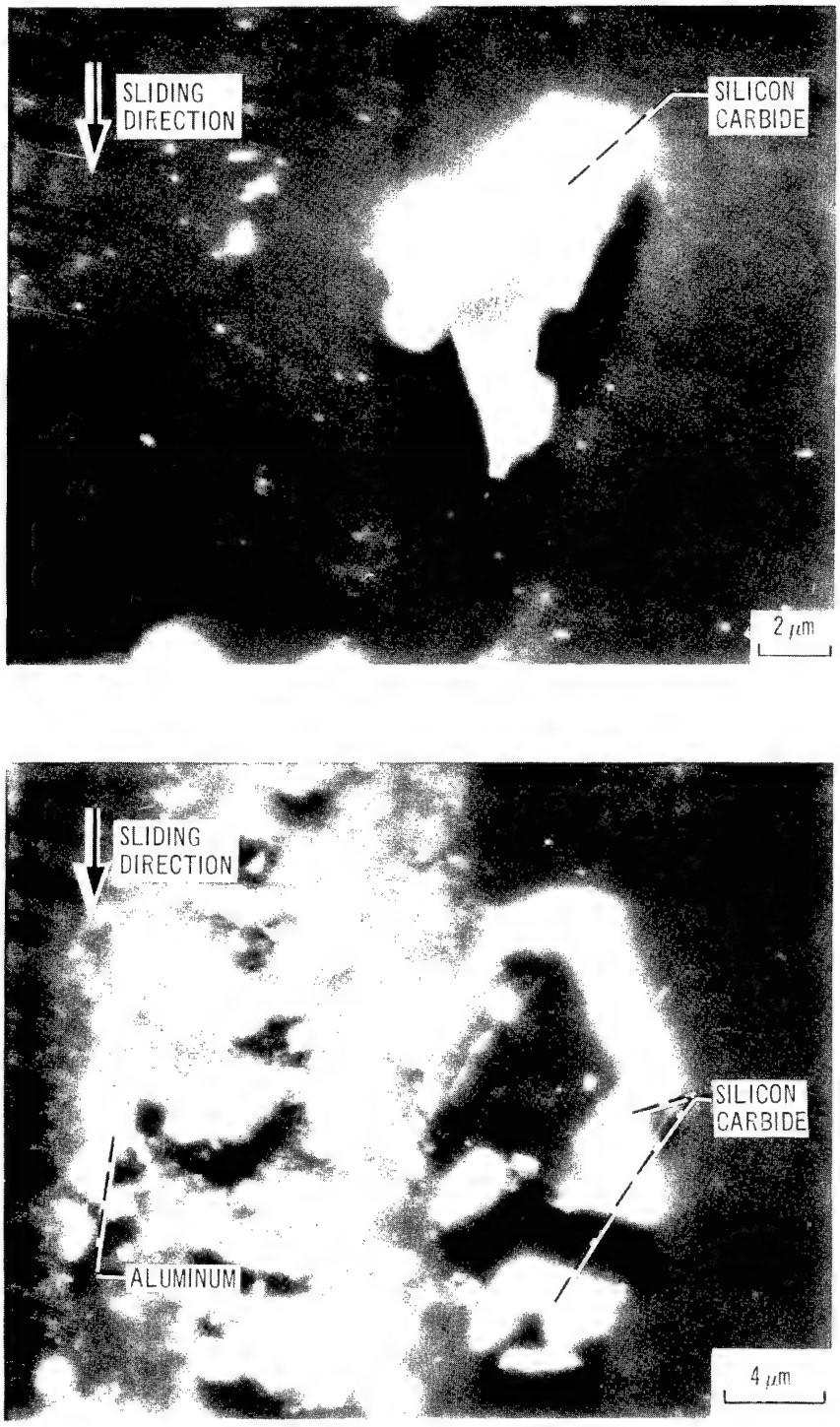

Figure 4. - Large wear debris of silicon carbide on SiC surface produced during sliding contact with aluminum rider. Ten passes on SiC (0001) surface; sliding direction, $<10\bar{1}0>$; sliding velocity, 3 mm/min; load, 30 g (0.29 N); temperature, 25° C; vacuum pressure, 10^{-8} Pa. (Scanning electron micrographs.)

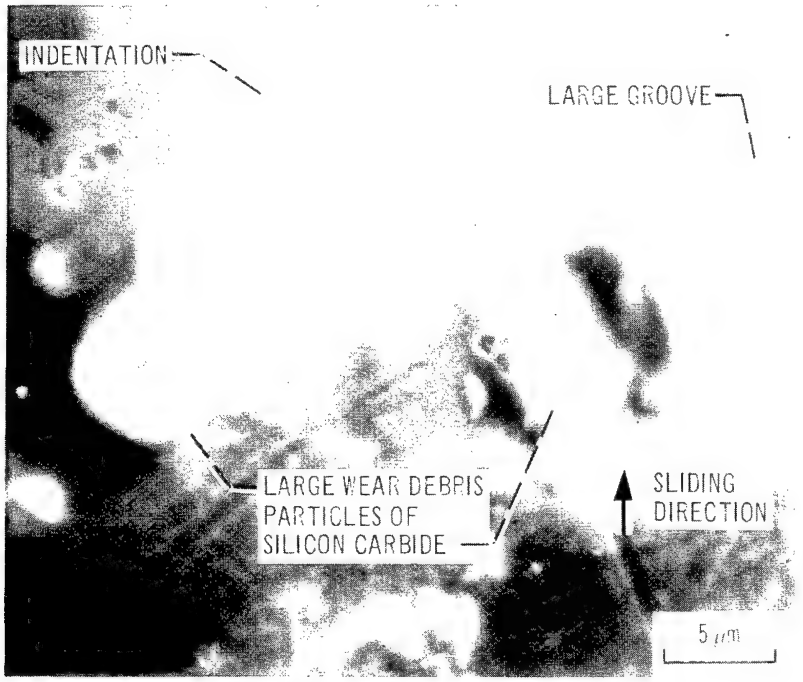

(a) Scanning electron micrograph.

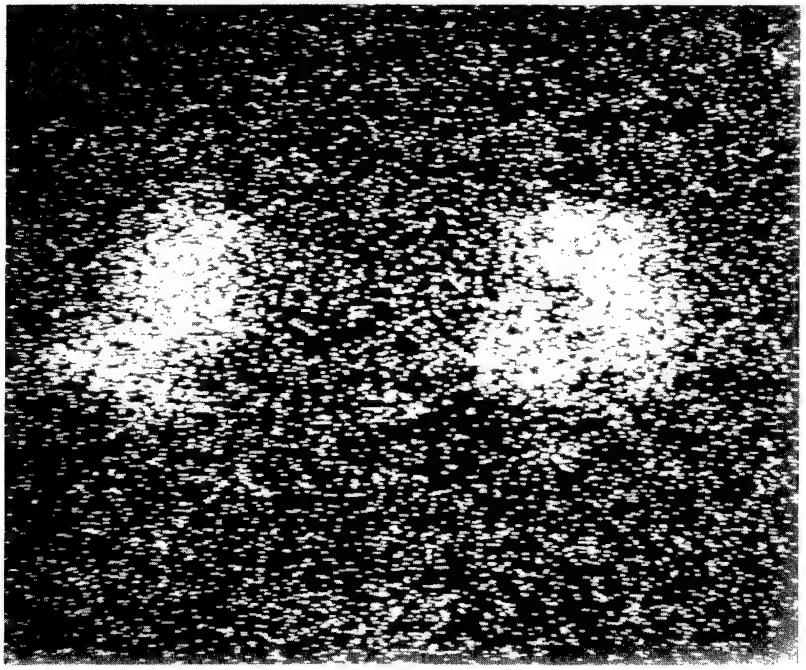

(b) Silicon K_α X-ray map of rhodium rider; 2.0×10^4 counts.

Figure 5. - Grooves and indentations on rhodium rider produced by silicon carbide wear debris during sliding contact. Ten passes on SiC (0001) surface; sliding direction, $<10\bar{1}0>$; sliding velocity, 3 mm/min; load, 30 g (0.29 N), temperature, 25° C; vacuum pressure, 10^{-8} Pa.

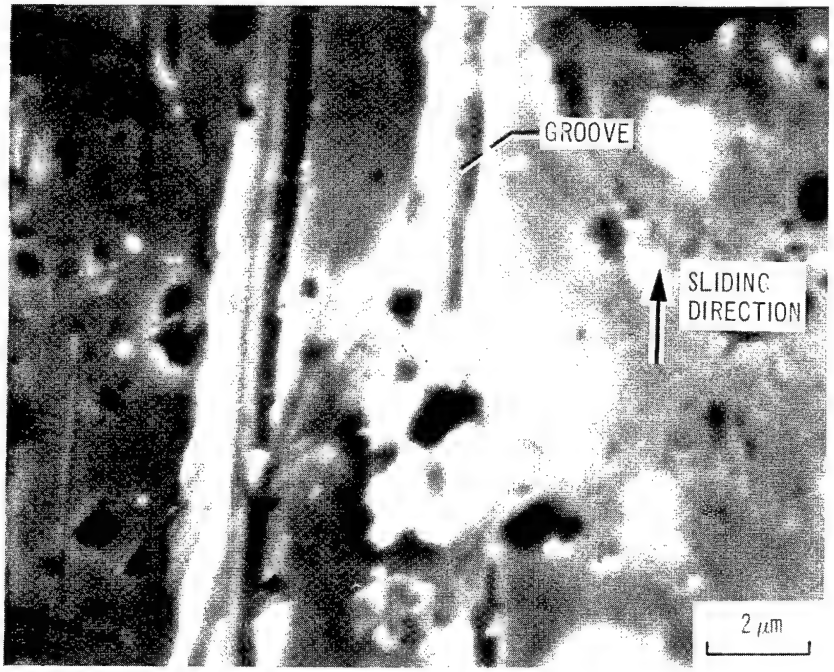

(a) Scanning electron micrograph.

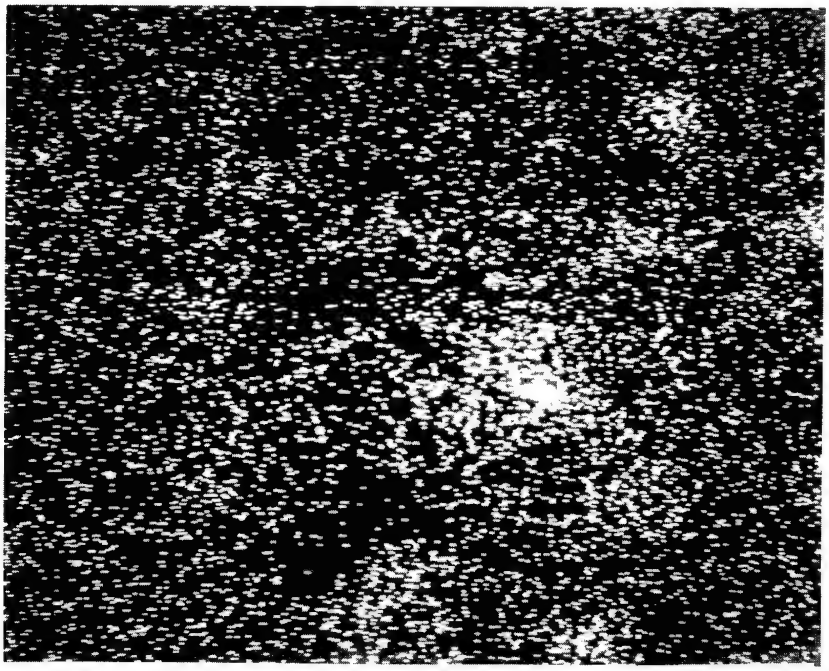

(b) Silicon K_α X-ray map of copper rider; 1.5×10^4 counts.

Figure 6. - Grooves on copper rider produced by scratching of silicon carbide wear debris during sliding contact. Ten passes on SiC (0001) surface; sliding direction, $<10\bar{1}0>$; sliding velocity, 3 mm/min; load, 30 g (0.29 N); temperature, 25° C; vacuum pressure, 10^{-8} Pa.

(a) Scanning electron micrograph.

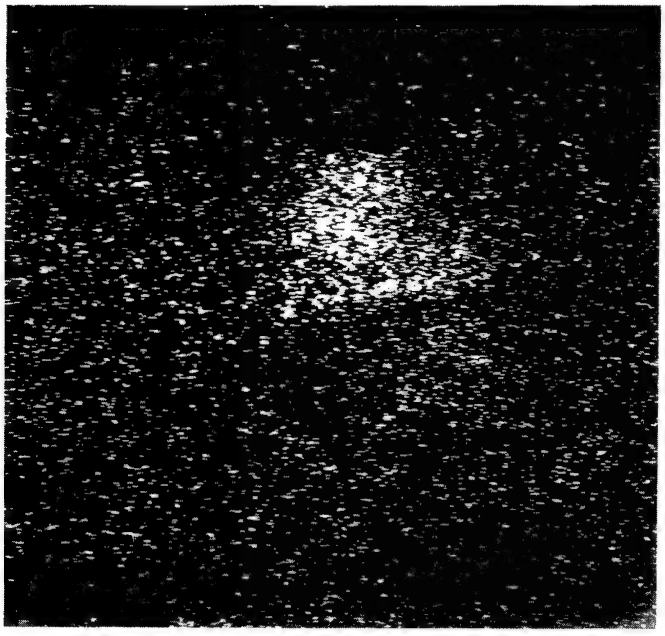

(b) Silicon K_α X-ray map of cobalt rider; 1.0×10^4 counts.

Figure 7. - Indentations on cobalt rider produced by rolling of silicon carbide wear debris during sliding contact. Ten passes on SiC (0001) surface; sliding direction, $<10\bar{1}0>$; sliding velocity, 3 mm/min; load, 30 g (0.29 N); temperature, 25° C; vacuum pressure, 10^{-8} Pa.

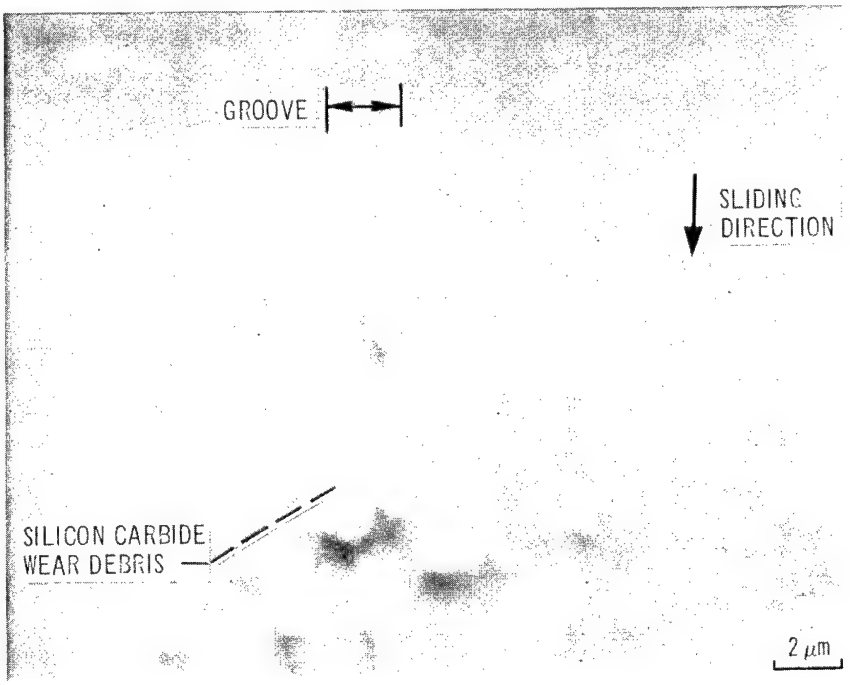

(a) Scanning electron micrograph.

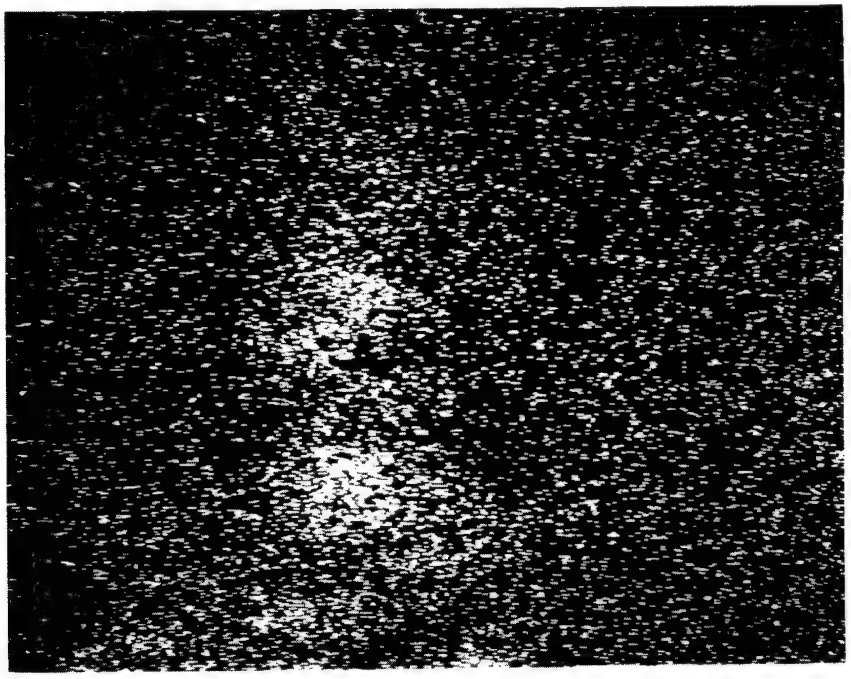

(b) Titanium K_α X-ray map of silicon carbide surface, 1.7×10^4 counts.

Figure 8. - Groove on silicon carbide produced by silicon carbide wear debris during sliding contact with titanium rider. Ten passes on SiC (0001) surface; sliding direction, $<10\bar{1}0>$; sliding velocity, 3 mm/min; load, 30 g (0.29 N); temperature, 25° C; vacuum pressure, 10^{-8} Pa.

(a) Aluminum.

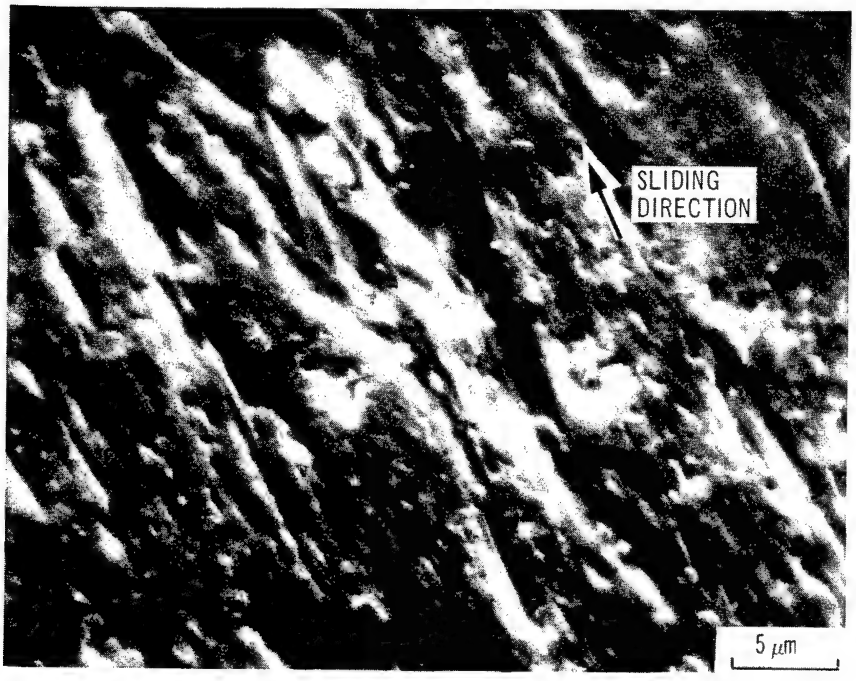

(b) Titanium.

Figure 9. - Wear scars on metal riders produced during sliding contact with silicon carbide. Ten passes on SiC (0001) surface; sliding direction, $<10\bar{1}0>$; sliding velocity, 3 mm/min; load, 30 g (0.29 N); temperature, 25° C; vacuum pressure, 10^{-8} Pa. (Scanning electron micrographs.)

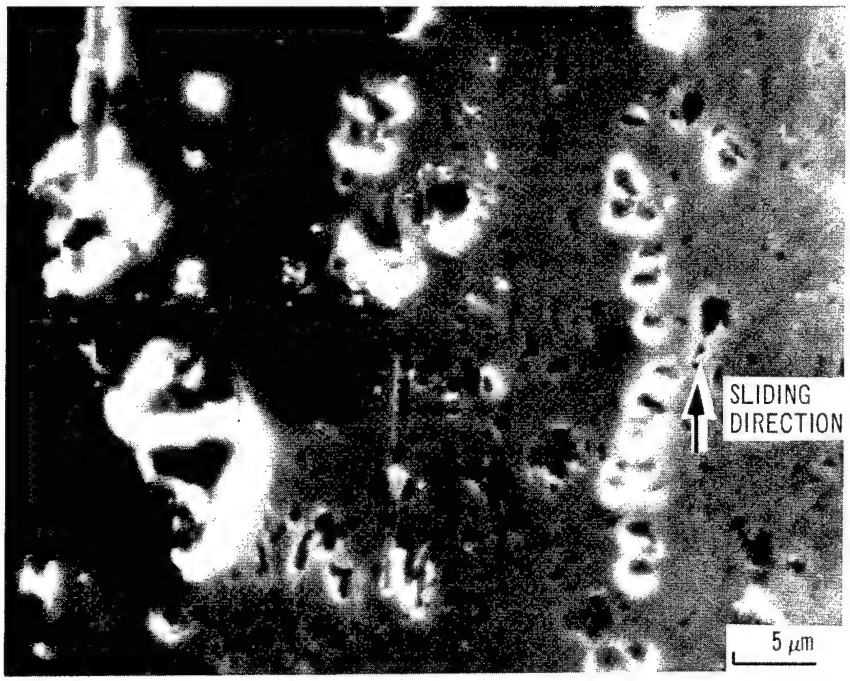

(c) Copper.

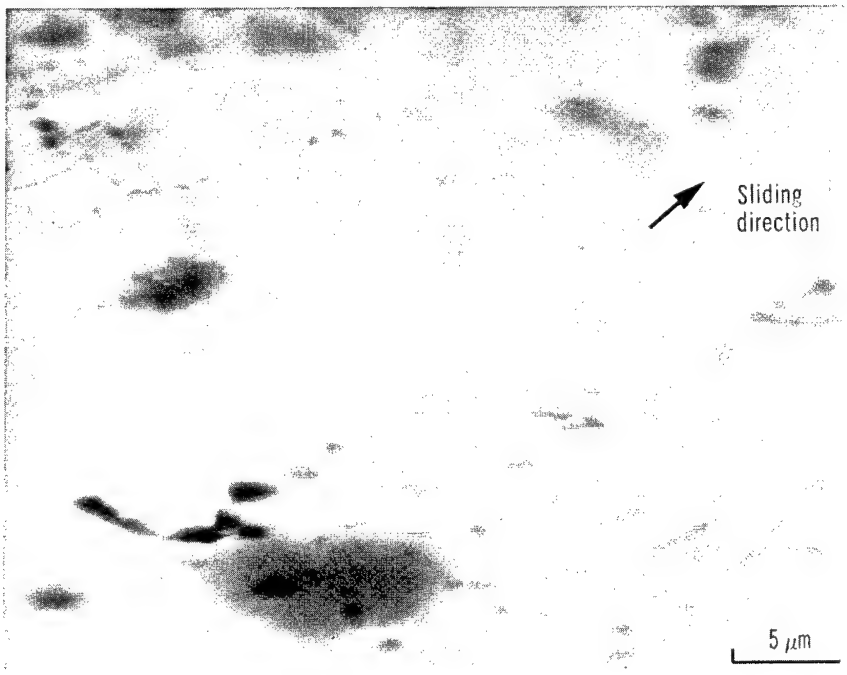

(d) Nickel.

Figure 9. - Continued.

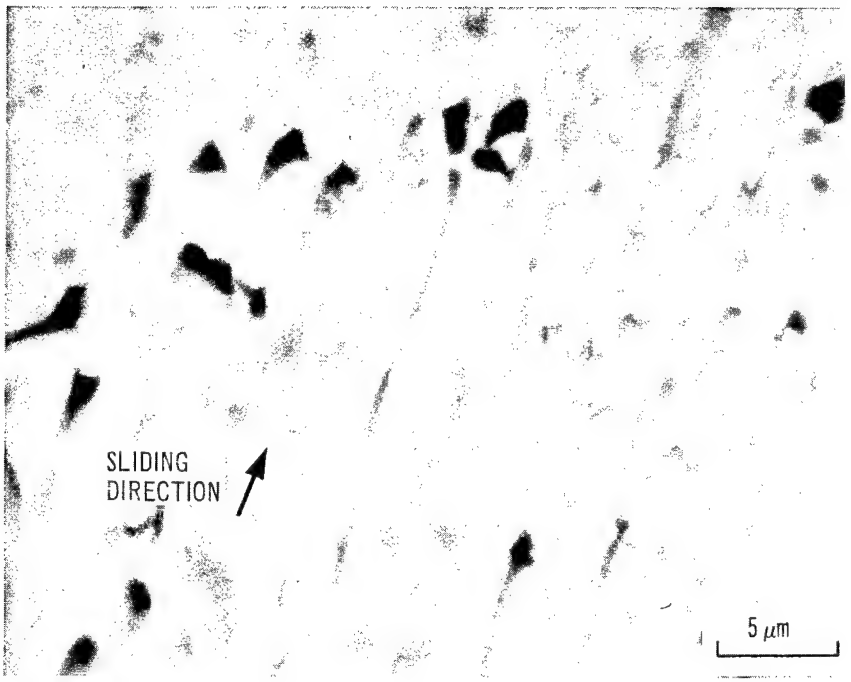

(e) Cobalt.

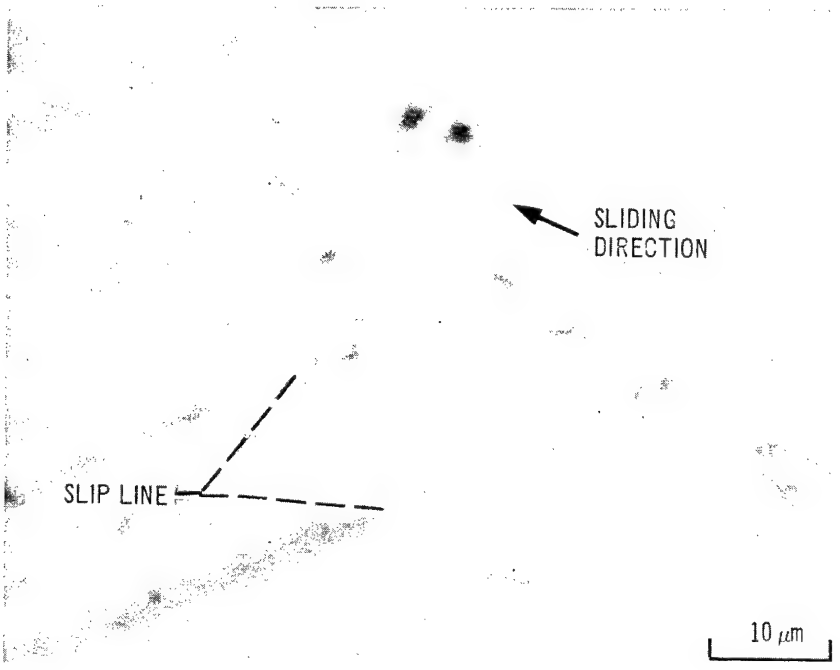

(f) Iron.

Figure 9. - Concluded.

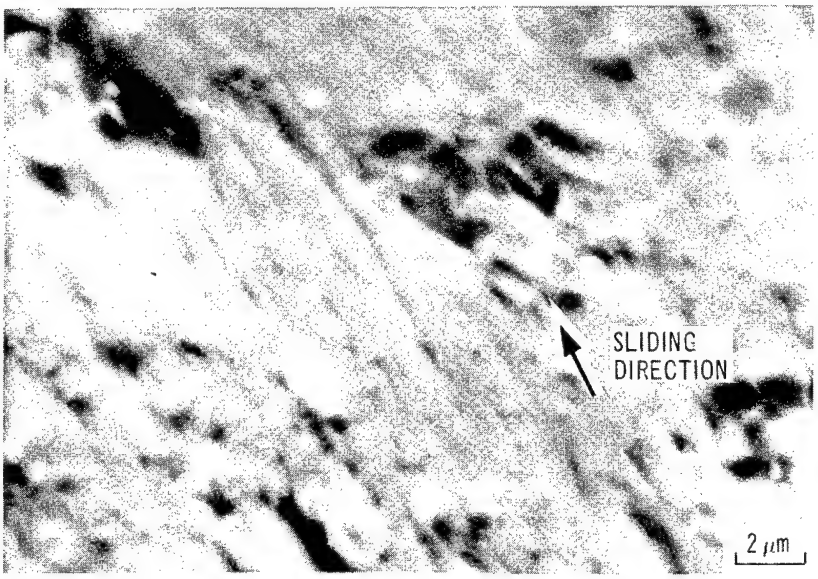

(a) Scanning electron micrograph.

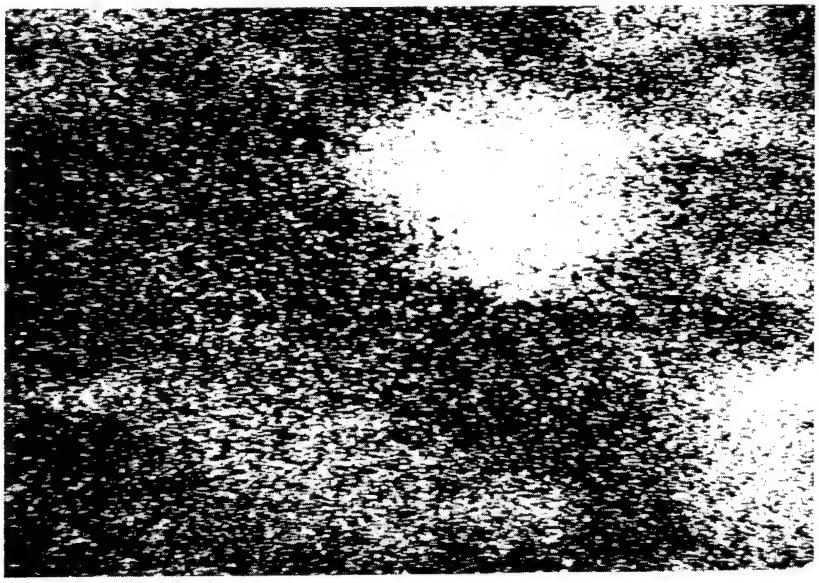

(b) Silicon K_α X-ray map of titanium rider; 3.0×10^4 counts.

Figure 10. - Rough surface of titanium rider showing large amount of silicon carbide transfer. Ten passes on SiC (0001) surface; sliding direction, $<10\bar{1}0>$; sliding velocity, 3 mm/min; load, 30 g (0.29 N); temperature, 25° C; vacuum pressure, 10^{-8} Pa.

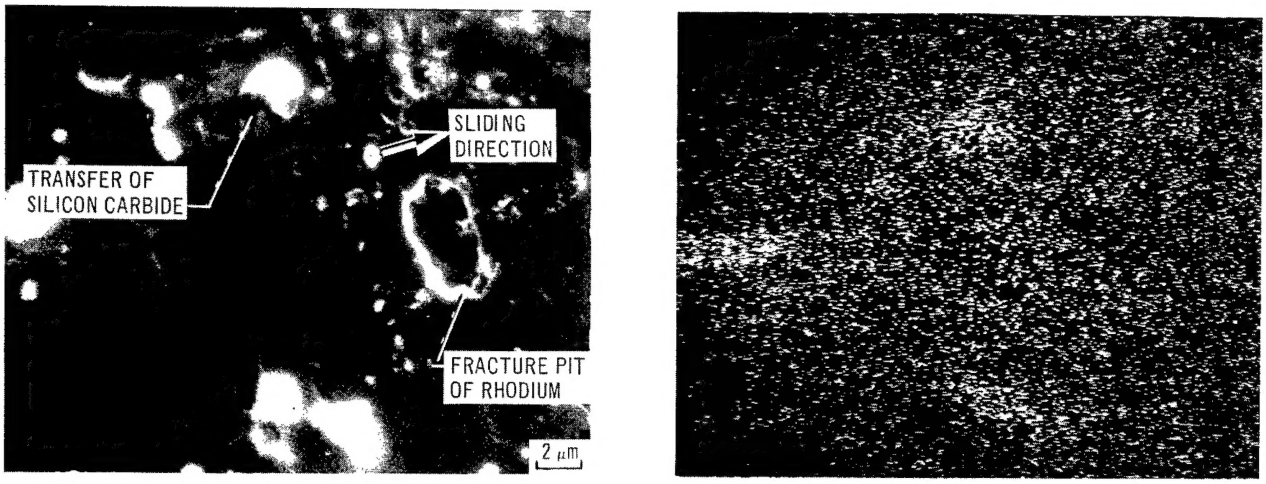

(a) Scanning electron micrograph and silicon Kα X-ray map of rhodium rider; 1.5×10^4 counts.

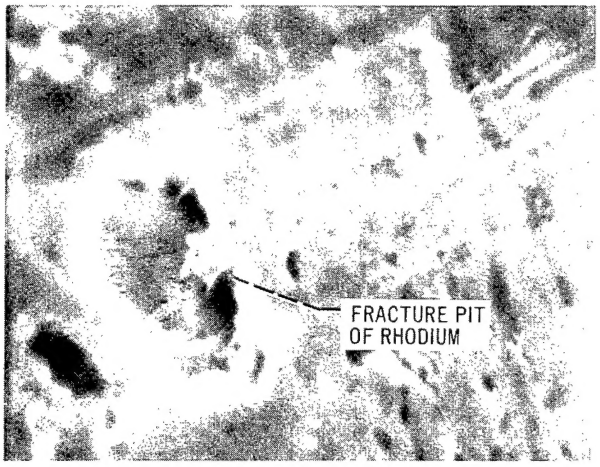

(b) Scanning electron micrograph (high magnification).

Figure 11. - Wear scar on rhodium rider showing grooves, indentations, and fracture. Ten passes on SiC (0001) surface; sliding direction, $<10\bar{1}0>$; sliding velocity, 3 mm/min; load, 30 g (0.29 N); temperature, 25° C; vacuum pressure, 10^{-8} Pa.

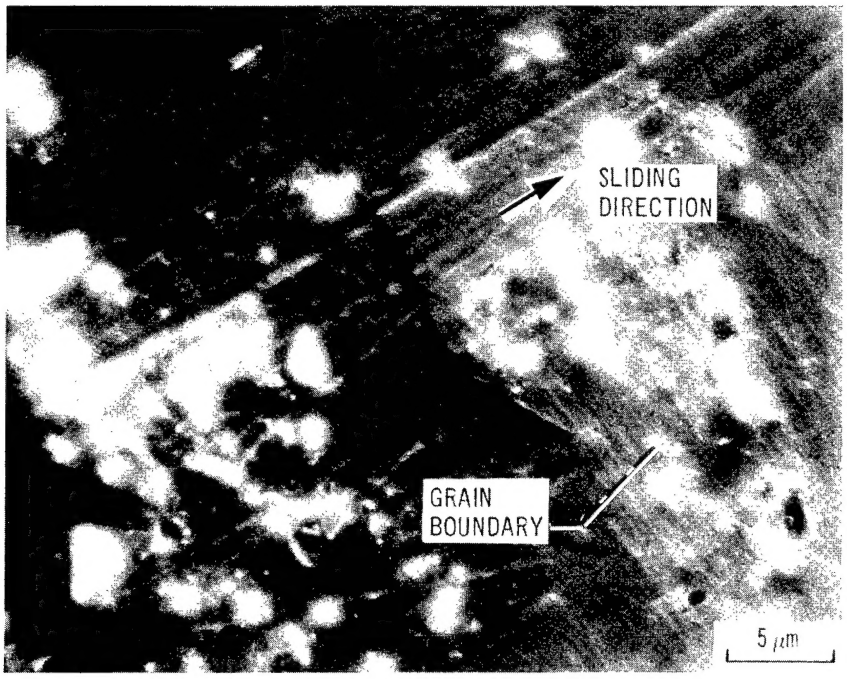

Figure 12. - Wear scar on rhodium rider showing cracks propogating along grain boundary. Three passes on SiC (0001) surface; sliding direction, <1010>; sliding velocity, 3 mm/min; load, 30 g (0.29 N) temperature, 25° C; vacuum pressure, 10^{-8} Pa.

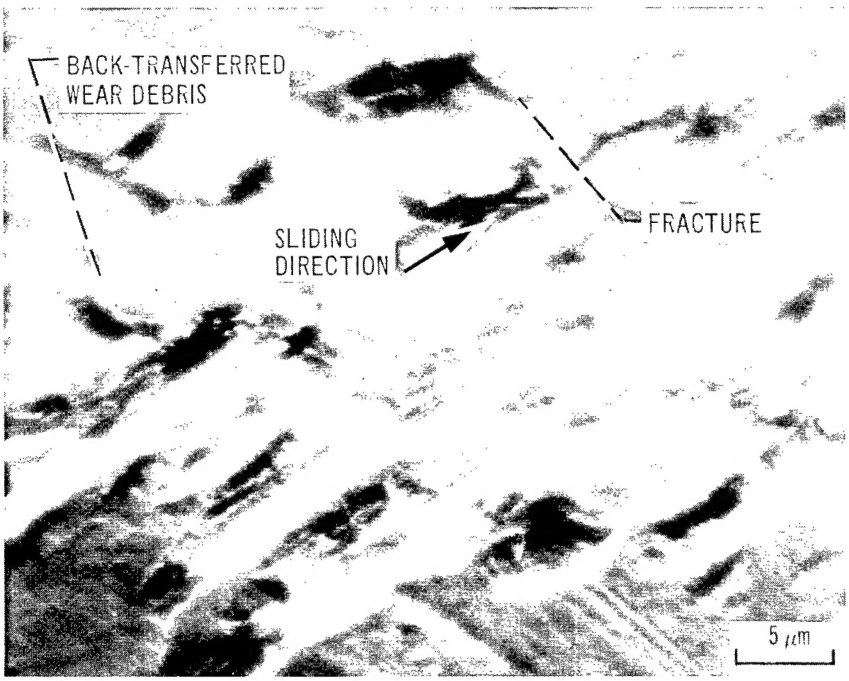

(a) After three passes.

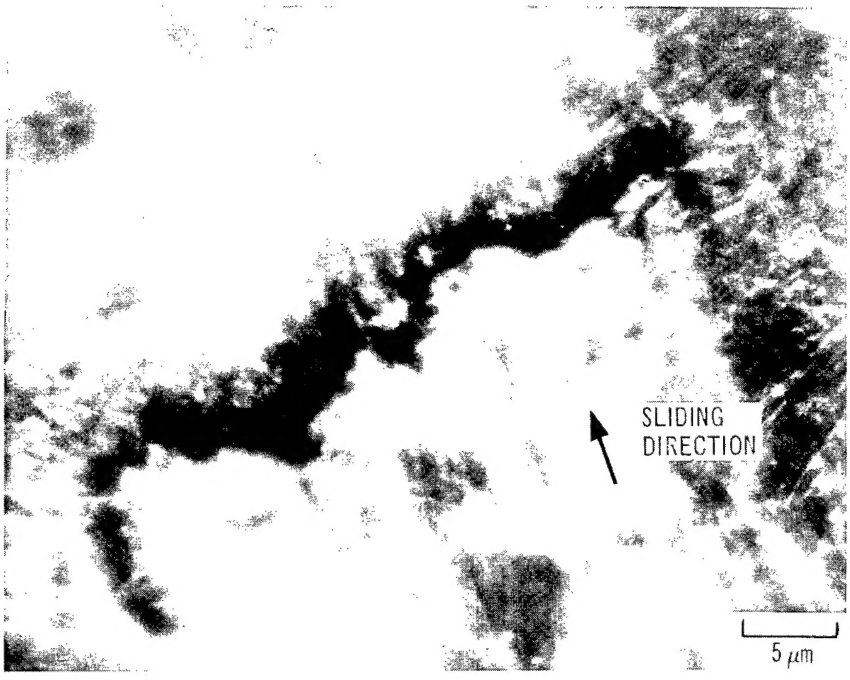

(b) After 10 passes.

Figure 13. - Tungsten rider wear scars produced during sliding contact with silicon carbide (0001) surface. Sliding direction, <10$\bar{1}$0>; sliding velocity, 3 mm/min; load, 30 g (0.29 N); temperature, 25° C; vacuum pressure, 10^{-8} Pa.

1. Report No. NASA TP-1198	2. Government Accession No.	3. Recipient's Catalog No.
4. Title and Subtitle WEAR OF SINGLE-CRYSTAL SILICON CARBIDE IN CONTACT WITH VARIOUS METALS IN VACUUM		5. Report Date April 1978 6. Performing Organization Code
7. Author(s) Kazuhisa Miyoshi and Donald H. Buckley		8. Performing Organization Report No. E-9360 10. Work Unit No. 506-16
9. Performing Organization Name and Address National Aeronautics and Space Administration Lewis Research Center Cleveland, Ohio 44135		11. Contract or Grant No. 13. Type of Report and Period Covered Technical Paper
12. Sponsoring Agency Name and Address National Aeronautics and Space Administration Washington, D.C. 20546		14. Sponsoring Agency Code

15. Supplementary Notes

16. Abstract

Sliding friction experiments were conducted in vacuum with single-crystal silicon carbide (0001) surface in contact with transition metals (tungsten, iron, rhodium, nickel, titanium, and cobalt), copper, and aluminum. The hexagon-shaped cracking and fracturing of silicon carbide that occurred is believed to be due to cleavages of both the prismatic and basal planes. The silicon carbide wear debris, which was produced by brittle fracture, slides or rolls on both the metal and silicon carbide and produces grooves and indentations on these surfaces. The wear scars of aluminum and titanium, which have much stronger chemical affinity for silicon and carbon, are generally rougher than those of the other metals. Fracturing and cracking along the grain boundary of rhodium and tungsten were observed. These may be primarily due to the greater shear moduli of the metals.

17. Key Words (Suggested by Author(s))	18. Distribution Statement		
Single-crystal silicon carbide; Metals; Auger; Wear; Fracture	Unclassified - unlimited STAR Category 27		
19. Security Classif. (of this report) Unclassified	20. Security Classif. (of this page) Unclassified	21. No. of Pages 23	22. Price* A02

* For sale by the National Technical Information Service, Springfield, Virginia 22161

NASA-Langley, 1978